

Highly resolved detection and selective focusing in a waveguide using the D.O.R.T. method

Nicolas Mordant, Claire Prada, and Mathias Fink

Laboratoire Ondes et Acoustique, Université Paris 7, CNRS UMR C7587, ESPCI, 10 rue Vauquelin, 75352, Paris Cedex 05, France

(Received 28 July 1998; accepted for publication 22 January 1999)

The D.O.R.T. method (French acronym for Decomposition of the Time Reversal Operator) is a scattering analysis technique using an array of transducers. The method is effective to achieve detection and selective focusing on pointlike scatterers through inhomogeneous media [J. Acoust. Soc. Am. **99**, 2067–2076 (1996)]. Laboratory measurements in a water waveguide are presented. Taking advantage of the multiple reflections at the interfaces of the guide, high resolution is achieved with the D.O.R.T. method. The separation of two scatterers and the selective focusing are obtained with a transverse resolution at least nine times better than the free-space limit prediction. The detection of a scatterer from the water/air interface of the guide is also achieved with high resolution (1/20 of the free space diffraction spot). The effect on the D.O.R.T. method of surface waves produced at one interface of the guide is measured. Finally, the impulse response function of each scatterer to the array is computed as a combination of the eigenvectors of the time-reversal operator obtained at each frequency. Using these impulse Green's functions, selective focusing with high temporal and spatial compression is performed. © 1999 Acoustical Society of America. [S0001-4966(99)00505-6]

PACS numbers: 43.30.Pc, 43.30.Re, 43.30.Gr [DLB]

INTRODUCTION

The problem of optimum signal transmission and source location in a waveguide has been the subject of many theoretical and experimental works. The propagation of an acoustic pulse inside a waveguide is a complex phenomenon. This complexity renders the detection and imaging process very difficult. Because of multiple path effects, the Green's function that is used in matched field processing is nontrivial and its calculation requires accurate knowledge of the medium. Several studies have shown how to take advantage of this complexity. In waveguide transmission, the guide can be considered as a linear filter. This concept can be applied in the ocean. Parvulescu *et al.*^{1,2} reported a matched filter experiment in the ocean between a source and a receiver. They recorded the reception of an impulsive transmission and replayed the time-reversed signal through the source. They obtained a high temporal compression, which was explained by the coherent recombination of the energy received over different multiple paths. They also showed high sensitivity to small displacements of the source, suggesting that this property should be used to locate the source.

The ability to achieve temporal and spatial focusing is even more striking in complex medium such as a chaotic reflecting cavity. C. Draeger *et al.*³ put this in evidence in a time-reversal experiment with a single source and a single receiver in silicone wafer.

As proposed by C. S. Clay and S. Li,^{4,5} the combination of array matched filter and time domain matched signal techniques improve the accuracy in source localization. They reported a laboratory experiment where they achieved focusing in the receive mode using the time-reversed version of the calculated impulse responses of the waveguide. They demonstrated an improvement of the spatial resolution due to the

multiple images of the receiver with respect to the waveguide interfaces. In these papers, focusing is explained in terms of matched signal: The waveguide plays the role of a correlator. The possibility to take advantage of the invariance of acoustic wave equation under time reversal in order to achieve spatial and temporal focusing arose afterward. In 1989, we built the first time-reversal mirror that was able to time reverse a wave field with an array of transducers.⁶ At the beginning, this system was aimed to compensate for distortions induced by sound speed fluctuations and for misalignment of the transducers in the array. In 1991, D. R. Jackson *et al.*⁷ showed that time-reversal mirror should be used in underwater sound to achieve highly resolved focusing. They provided a theoretical analysis of the time-reversal process in a water channel.

Focusing experiments inside a water waveguide with a time-reversal mirror were first achieved in 1995 by P. Roux *et al.*^{8,9} They demonstrated how to refocus an incident acoustic field back to its origin and to achieve high temporal and spatial compression by time reversal of the wave field. They obtained a 6-dB focal width that was nine times narrower than the free-space diffraction limit prediction. In 1996, an impressive experiment was realized by Kuperman and his team in the Mediterranean Sea.¹⁰ They have implemented a time-reversal mirror and have shown that the time-reversal process allows refocusing at 6-km distance in a 120-m deep water channel.

In the abovementioned papers, only transmission from sources to receivers is considered. A natural question is how to use this super focusing property to detect scatterers in an echographic mode. This question is of practical concern for nondestructive evaluation as well as underwater acoustics. In echographic mode, the signal reflected from a scatterer is

extremely complex for it has undergone a double path through the guide. We propose to apply the D.O.R.T. method to this particular problem. This method was first presented in 1994 in a paper entitled ‘‘Eigenmodes of the time-reversal operator: A solution to selective focusing in multiple target media.’’¹¹ Since then it has been used to make detection and selective focusing through aberrating media,^{12,13} and also to separate Lamb modes propagating around a thin hollow cylinder.¹⁴ As will be shown in this paper, the method can also take advantage of the matched filter property of the waveguide in order to separate the echoes from different scatterers with high resolution.

In Sec. I, the principle of the D.O.R.T. method is recalled; then an example of highly resolved detection and selective focusing in a water waveguide is presented. The detection of a scatterer placed near an interface of the guide is studied in Sec. II.

In Sec. III, the imaging problem is addressed by adding an *a priori* knowledge on the guide. The field produced by transmission of the conjugate eigenvectors is calculated with a simple ray model where the guide parameters are determined by an iterative optimization procedure.

The consequences of fluctuations of the medium on the performance of the D.O.R.T. method are studied in Sec. IV. The considered waveguide is a water layer delimited by steel and air interfaces. Surface waves are produced at the water/air interface.

In Secs. I–IV, the analysis of the transfer function is done at a single frequency. In the last section, it is shown that in some cases the eigenvectors obtained at each frequency can be combined to obtain the time domain Green’s function for each scatterer.

I. SELECTIVE HIGHLY RESOLVED FOCUSING IN A WAVEGUIDE

The D.O.R.T. method was widely described in several papers.^{13,14} For the detection part it consists in the following steps. First, the inter-element impulse response functions, $k_{lm}(t)$, are measured. Second, the transfer matrix is calculated at one chosen frequency (more often the central frequency of the transducers). Finally, the time-reversal operator, $K^*(\omega)K(\omega)$, is diagonalized. In practice, it is convenient to calculate the singular value decomposition of the transfer matrix: $K(\omega) = U(\omega)\Lambda(\omega)V^+(\omega)$, where $\Lambda(\omega)$ is a real diagonal matrix of the singular values, and $U(\omega)$ and $V(\omega)$ are unitary matrices. The eigenvalues of

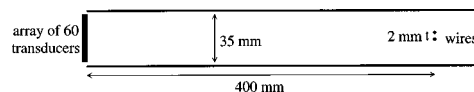


FIG. 1. Geometry of the experiment.

$K^*(\omega)K(\omega)$ are the squares of the singular values of $K(\omega)$, and its eigenvectors are the columns of $V(\omega)$. We shall use this decomposition in the following.

For pointlike scatterers, the general result that was shown is that the number of ‘‘nonzero’’ singular values is equal to the number of well-resolved scatterers. Furthermore, if the scatterers have different ‘‘apparent’’ reflectivities, each eigenvector provides the phase and amplitude to be applied to the transducers in order to focus on one particular scatterer. For the detection part, the D.O.R.T. method shares some of the principles of eigenvector decomposition techniques that are used in passive source detection,^{15,16} however, it should not be considered as a competing technique as it is active and deterministic.

A. Experimental geometry

The experiment is performed in a two-dimensional water waveguide, delimited by two water/steel plane interfaces. In a good approximation, the reflections at the interfaces can be considered as total. The water layer is 35 mm thick. The array consists of 60 transducers with a central frequency of 1.5 MHz, it spans the whole height of the guide with a pitch equal to 0.58 mm. The scatterers are two wires of diameters 0.1 mm and 0.2 mm, spaced 2 mm and placed perpendicular to the array axis at a distance of 400 mm (Fig. 1). As the average wavelength is 1 mm, both wires behave almost like point scatterers. For this range and this frequency, the free-space diffraction focal width is 12 mm so that the two wires are not resolved by the system.

The echographic signals recorded after a pulse is applied to one transducer of the array are very complex with low signal-to-noise ratio. The inter-element response $k_{28\ 40}(t)$ is a typical example (Fig. 2). After approximately five reflections at the interfaces, the signal can no longer be distinguished from noise. The echoes of the two wires are superimposed and cannot be separated in a simple manner.

B. Eigenvectors and singular values

The 60×60 impulse response functions are measured and the transfer matrix is calculated at frequency 1.5 MHz. Decomposition reveals two singular values that are separated

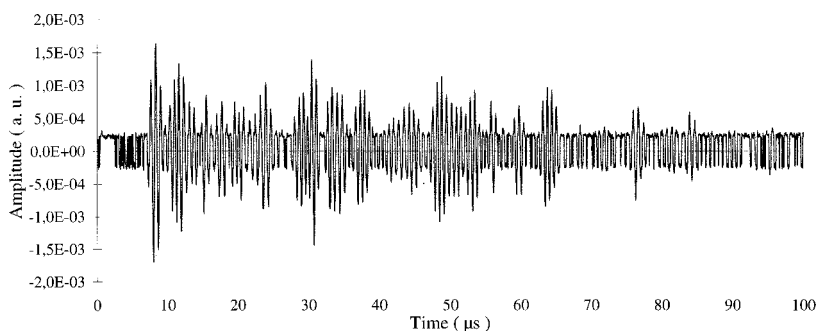


FIG. 2. Typical echo of the wires: inter-element impulse responses $k_{28\ 40}(t)$.

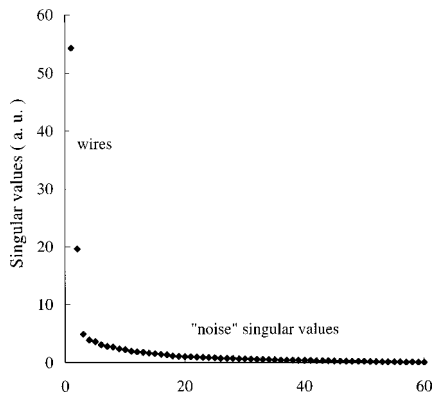


FIG. 3. Singular values of the transfer matrix calculated at 1.5 MHz.

from the 58 “noise” singular values (Fig. 3). The “noise” singular values are partly explained by electronic and quantization noises. However, different second order acoustical phenomena that are not taken into account in the model probably contribute to these singular values: among them, the defects of the interfaces, the elastic responses of the wires, the multiple echoes between the wires, and also coupling between the transducers.

C. Selective focusing in monochromatic mode

The eigenvectors V_1 and V_2 have a complicated phase and amplitude distribution and it is impossible to tell to which scatterer each of them corresponds. These distributions are applied to the array of transducers. Namely, if $V_1 = (A_1 e^{i\varphi_1}, A_2 e^{i\varphi_2}, \dots, A_n e^{i\varphi_n})$ is the first eigenvector, then the signal $s_p(t) = A_p \cos(\omega t - \varphi_p)$ is applied to transducer number p . A needle probe is used to scan the so produced pressure field across the guide at the range of the wires (Fig. 4). For each eigenvector, the wave is focused at the position of one wire. In both cases the residual level is lower than -18 dB and the -6 dB focal width is 1.4 m. In fact, the width is overestimated because the width of the probe is 0.5 mm, and the real focal width is probably around 1.2 m which is ten times thinner than the theoretical free-space focal width.

For comparison, the same experiment is achieved after removing the guide. In this case the wires are not resolved and only the first singular value is significant. The pressure pattern is measured for transmission of the first eigenvector,

and the focal width is 13 mm (Fig. 4). Consequently, the guide allows us to achieve a focusing at least 10 times thinner than in free space. The angular directivity of each transducer limits the number of reflections at the guide interfaces that can be recorded. This induces an apodization of the virtual array made of the set of images of the real one. Taking this phenomenon into account, the focal width roughly corresponds to a virtual aperture consisting of eight pairs of images of the array.

II. DETECTION NEAR THE INTERFACE

In many problems, the detection of a defect near an interface is difficult, especially if the reflectivity coefficient of the interface is close to -1 , which is the case for the water/air interface. Indeed, in this situation, the virtual image of the defect with respect to the interface behaves as a source in opposite phase with the defect. The real source and the virtual source interfere in a destructive way so that the reflected signal is very low. Here we analyze the ability of the D.O.R.T. method to detect a wire that is close to a water/air interface.

The experiment is done in a water waveguide of 35-mm width limited by air at the surface and steel at the bottom. A wire of 0.2 mm diameter is placed inside the guide at 400 mm from the array. The wire is moved step by step from the bottom to the surface and for each position the transfer matrix is measured and decomposed. The two first singular values are displayed versus the distance to the surface (Fig. 5). The first singular value represents the signal level and the second one represents the noise level. When the wire reaches the bottom, the singular value increases rapidly by a factor of 2: The echoes from the scatterer and from its image add constructively. Conversely, when the wire gets to the surface the singular value decreases rapidly. It remains well separated from the noise singular values until the distance between the wire and the interface reaches $\lambda/5$.

To illustrate the role played by multiple reflections at the interfaces, a simple model is used to calculate the theoretical singular values for different numbers of reflections. The reflection coefficients are taken equal to 1 at the bottom and equal to -1 at the surface. According to the theory,^{13,14} the singular value of the transfer matrix is $\lambda_1 = c \sum_l |H_l|^2$, where c is the reflectivity coefficient of the scatterer and H_l is the response from the scatterer to transducer number l . For a

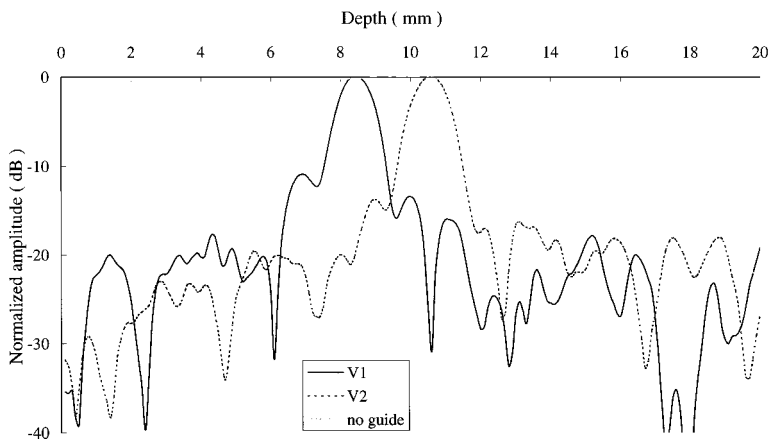


FIG. 4. Pressure pattern measured across the guide at the range of the wires after transmission of the eigenvectors. First (solid) and second (dot) eigenvectors obtained with the guide, first (gray) eigenvector without the guide.

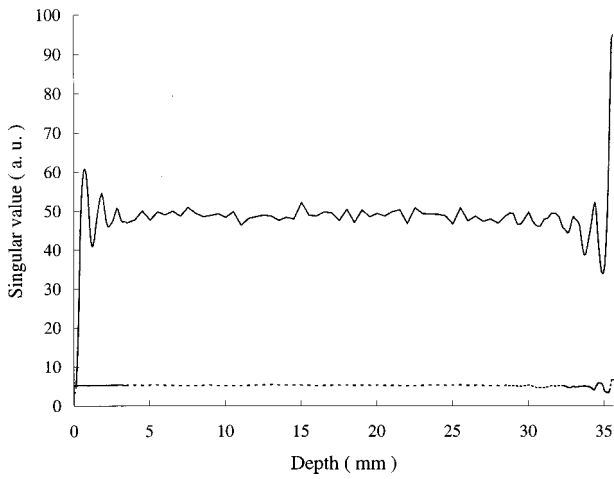


FIG. 5. Experiment: Dependence of the singular values of the transfer matrix versus the distance to the surface (solid: first, dashed: second).

scatterer close to the upper interface the images have to be taken into account by pairs: (S, I_1) , (I_{-1}, I_{-2}) , (I_2, I_3) , and so on. Each pair corresponds to adjacent acoustic paths (Fig. 6).

There is a qualitative agreement between theoretical (Fig. 7) and experimental curves (Fig. 5). The abovementioned phenomenon can be seen: The singular value decreases to zero when the wire reaches the surface. Again, the more reflections are taken into account the closer to the surface the wire can be detected. The minimum distance to the surface under which the wire is no longer detected is the distance where the first singular value is at the level of noise singular values. It depends on the number of images that are taken into account. For example, assuming that the noise singular values level is 500 (this corresponds roughly to the experimental noise singular values), for one image the minimum distance is 2 mm, for three images it is 0.4 mm, and for five images it is less than 0.2 mm. This is another illustration of the ability of the D.O.R.T. method to provide high resolution by taking advantage of multiple paths.

III. IMAGING THE SCATTERERS

In the experiment of Sec. I, the eigenvectors were used to focus selectively on each scatterer. Of course, this procedure is not sufficient to make an image or a localization of the scatterers. Imaging requires us to backpropagate numerically the data with an appropriate beamformer, which assumes a precise knowledge of the parameters of the

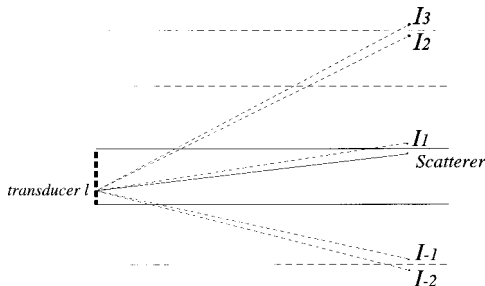


FIG. 6. Pairs of images used to calculate the singular values for a scatterer close to the surface.

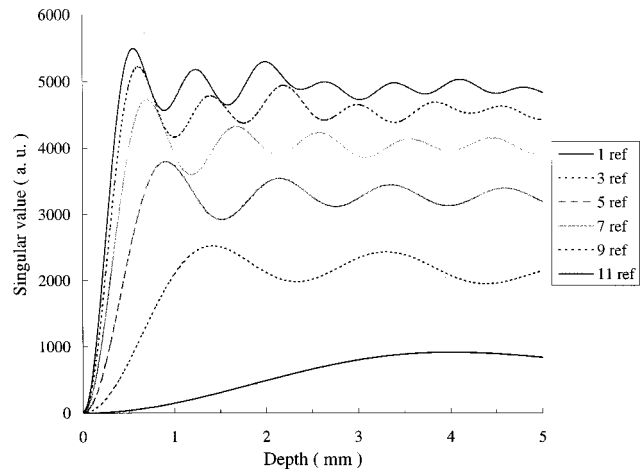


FIG. 7. Theoretical first singular value as a function of the distance to the interface calculated for different numbers of reflections at the interface.

waveguide.¹⁷ Here, we give a simple example using an optimization procedure to approximate parameters of the guide. The water guide is delimited by two parallel water/steel interfaces as in Sec. I. In a first approximation, the distance between the interfaces is $H=35$ mm, the transducers array is perpendicular to the guide ($\alpha=0^\circ$), and the distance from the center of the array to one interface is $d_0=17.5$ mm. Four scatterers of diameters up to 0.2 mm are placed at range $r_1=r_2=388$ mm, $r_3=r_4=398$ mm, and depth $h_1=12$ mm, $h_2=26$ mm, $h_3=17$ mm, and $h_4=22$ mm (Fig. 8). At 1.5 MHz, the theoretical free space focal spot is 12 mm in the transverse direction and 900 mm in range. Consequently, the wires are not resolved in a classical monochromatic approach.

The singular value decomposition of the transfer matrix is calculated at frequency 1.5 MHz. Four singular values are separated from the noise singular values, which reveals the presence of the four scatterers (Fig. 9). However, at this stage it is impossible to tell to which wire each eigenvector corresponds. To localize the wires, it is necessary to backpropagate the eigenvectors in the modeled waveguide.

A. Optimization of the guide parameters

Since the measurement of the parameters of the guide is not precise enough to backpropagate numerically the eigenvectors, we developed a self-adaptive method to optimize the values of the three parameters. A calibration wire is placed half-way between the four wires and the array of transducers. The distance between the reference and the targets is long enough so that the last measurable echo from the reference wire arrives before the first echo from the four wires.

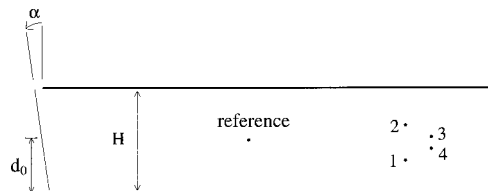


FIG. 8. Experimental setup and parameters used in the optimization procedure.

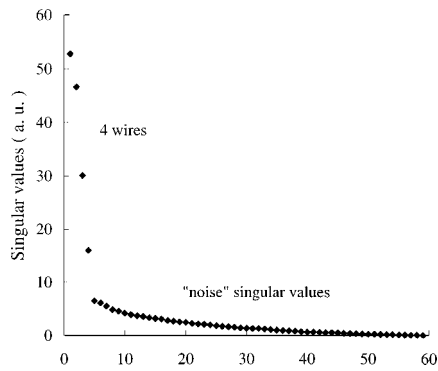


FIG. 9. Singular values of the transfer matrix obtained with the four wires.

The inter-element impulse responses of this wire are measured and the first eigenvector of the corresponding time reversal operator is calculated. As we know from the preceding results, the transmission of this eigenvector focuses on the reference wire. Thus the idea is to calculate the field produced by transmission of this eigenvector at the depth of the reference wire and to maximize the quality of the focusing. The parameters H , d_0 , and α are varied until the best focusing is obtained. Namely, the function to be maximized is

$$M_P = \frac{\max_D(|P(\alpha, H, d_0)|)}{\text{mean}_D(|P(\alpha, H, d_0)|)},$$

where D is the section of the guide at the range of the reference wire, and P is the pressure field calculated by transmission of the first eigenvector. This eigenvector is obtained taking into account all the measurable reflections. In order to avoid the problem of secondary maxima, backpropagation is first computed taking into account only two reflections on the guide interfaces. With fewer reflections the focal width is larger and the absolute maximum is easier to localize. Once the best parameters are obtained for two reflections, the procedure is iterated starting from the new parameters and adding one more reflections at each step. This process is iterated until the parameters converge.

After such an optimization of the focused pattern, the parameters are found to be $H = 34.77 \text{ mm} \pm 0.05 \text{ mm}$, $\alpha = 0.27^\circ \pm 0.01^\circ$, and the position of the array center $d_0 = 17.77 \text{ mm} \pm 0.05 \text{ mm}$.

B. Images provided by each eigenvector

The estimated values of the parameters H , d_0 , and α are used to calculate the pressure patterns for transmission of eigenvectors 1 to 4 corresponding to the responses of the four wires. The images are calculated in the range 375 mm to 414 mm on the whole height of the guide. Each eigenvector leads to a focusing at the position of one of the wire (Fig. 10). The resolution at -6 dB is 1.2 mm in depth and 10 mm in range, which corresponds to an effective aperture of 595 mm. The level of the side lobes reaches -4 dB . The four scatterers are well separated in this decomposition.

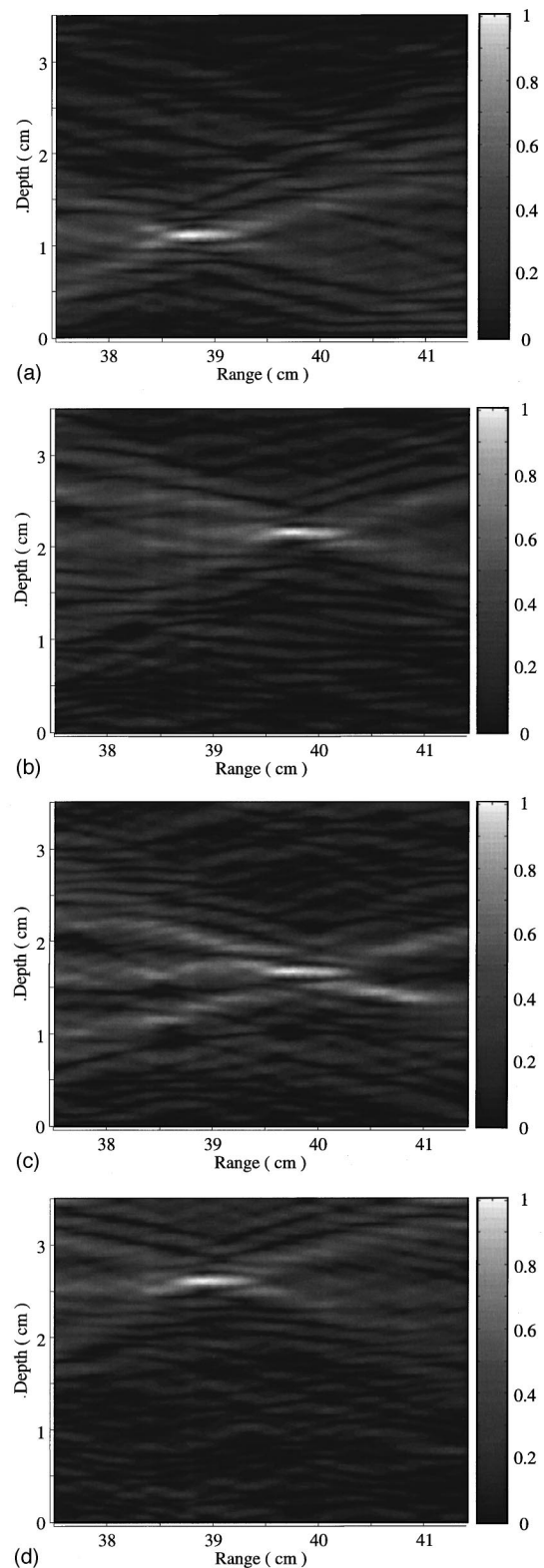


FIG. 10. Pressure field calculated by numerical propagation of eigenvectors 1 to 4.

C. Comparison with phase conjugation

To illustrate the efficiency of this method, we calculate the image obtained by the phase conjugation of an echo of the wires. As explained in different papers,^{6,7,11} the phase conjugate of an echo of the wires should refocus on each wire simultaneously, the amplitude of each focal spot de-

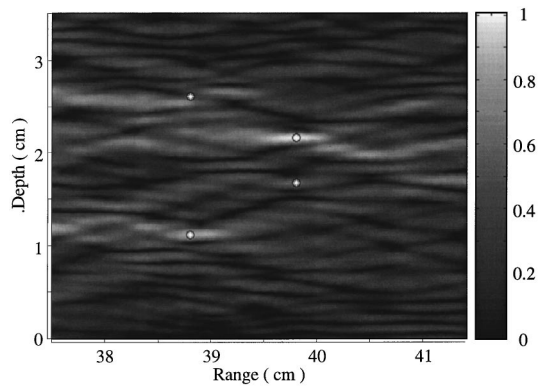


FIG. 11. Pressure field calculated by numerical propagation of the phase conjugated of the response of the wires obtained after transmission by ten elements in the center of the transducer array.

pending on the first insonification, and on the apparent reflectivity of the wires. In order to increase the signal-to-noise ratio, we choose to insonify the wires with ten adjacent transducers in the middle of the array. The Fourier component of the received echo is calculated at 1.5 MHz. This provides a complex vector V that is phase conjugated and numerically transmitted in the modeled wave guide.

On the phase conjugate image (Fig. 11), only the first and second most reflective wires can be distinguished. The energy refocused on the two other wires is at the same level as secondary lobes and thus cannot be distinguished. This result illustrates the efficiency of the D.O.R.T. method to detect weak scatterers among stronger ones, and thus to find more details of the scattering medium.

IV. STUDY OF A TIME VARYING WAVEGUIDE

To analyze the robustness of the method, we now propose to make measurements in a steel/water/air waveguide in the presence of surface waves. We study the dependence of the singular values distribution and the focusing obtained by transmission of the eigenvectors with respect to the root mean square height of the waves.

A vertical plate with horizontal oscillations at 6 Hz produces the surface waves. This displacement produces waves of typical wavelength of 30 mm. The height of the waves is varied using a diaphragm placed between the plate and the

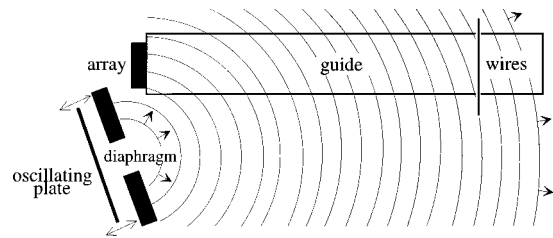


FIG. 12. Experimental setup built to produce surface waves.

guide (Fig. 12). A transducer put on the bottom and focused at the surface measures the time of flight to the surface, which provides the height of the waves. The root mean square height h_{rms} of the waves is varied from 0 to 1.7 mm. This corresponds to $0 < kh_{\text{rms}} < 10$. A copper wire and a tungsten wire of diameter 0.2 mm are placed at 500 mm from the array and spaced 5 mm.

For a given wave height, the transfer matrix K is measured and decomposed. While kh_{rms} is lower than 1.5, the two singular values corresponding to the wires are well separated from noise singular values. For $kh_{\text{rms}} = 1.5$, the two first eigenvectors were transmitted into the guide and the field measured at range 500 mm (Fig. 13). The eigenvectors focus at the position of the wires, however, the main lobes are approximately 1.6 times larger and the residual level twice higher than in the absence of waves (see Fig. 4).

At this stage, it is important to recall that the measurement of the matrix K takes 5 min. For our system the matrix is measured column by column so that each column corresponds to one realization of the medium. Consequently, the transfer matrix K corresponds to a sort of average medium. This may partly explain why the result of the backpropagation is good for one realization of the matrix K .

For higher waves, it is necessary to average the inter-element impulse responses over several realizations. The singular values of the ten times averaged matrix K_{10} are calculated for h_{rms} varying from 0 to 1.7 mm. The two greatest singular values decrease rapidly with the height of the waves while the noise singular values increase (Fig. 14). In fact, the main effect of the averaging is to lower the ‘noise’ singular values so that the signal singular values better emerge from noise. This phenomenon is illustrated in the case of $h_{\text{rms}} = 1.7$ mm ($kh_{\text{rms}} = 10$). The results obtained with one real-

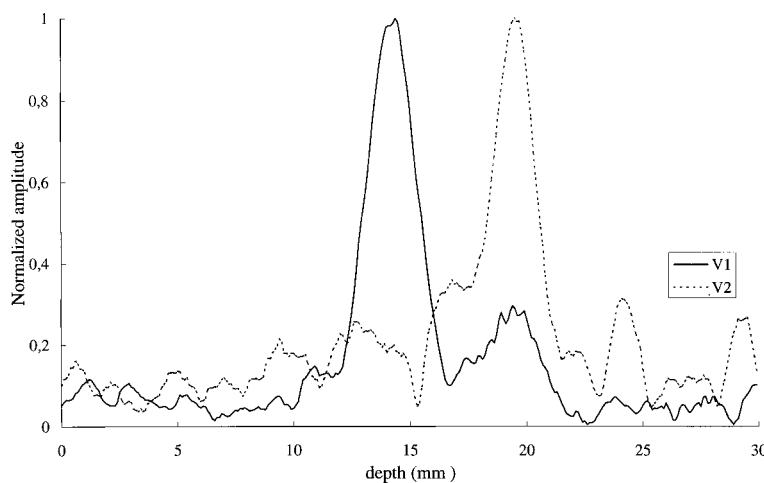


FIG. 13. Pressure field measured for transmission of eigenvectors 1 and 2 calculated with a nonaveraged transfer matrix obtained with surface waves of $h_{\text{rms}} = 0.23$ mm.

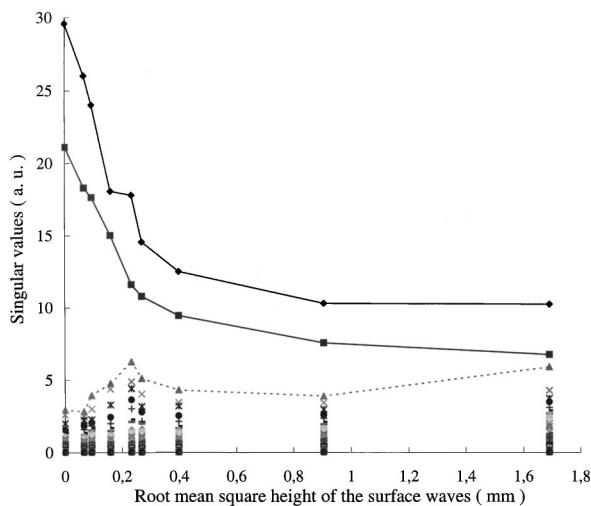


FIG. 14. Singular values of the ten times average transfer matrix versus the root mean square height of the waves (\blacklozenge first, \blacktriangle second, \blacksquare third).

ization of the inter-element impulse responses (matrix K_1) and with the average of ten realizations (matrix K_{10}) are compared. The corresponding eigenvectors are transmitted into the guide and the so-produced field measured. For the first eigenvector, the averaging does not make any significant difference on the focus pattern [Fig. 15(a)]. This is probably due to the fact that the signal corresponding to the strongest

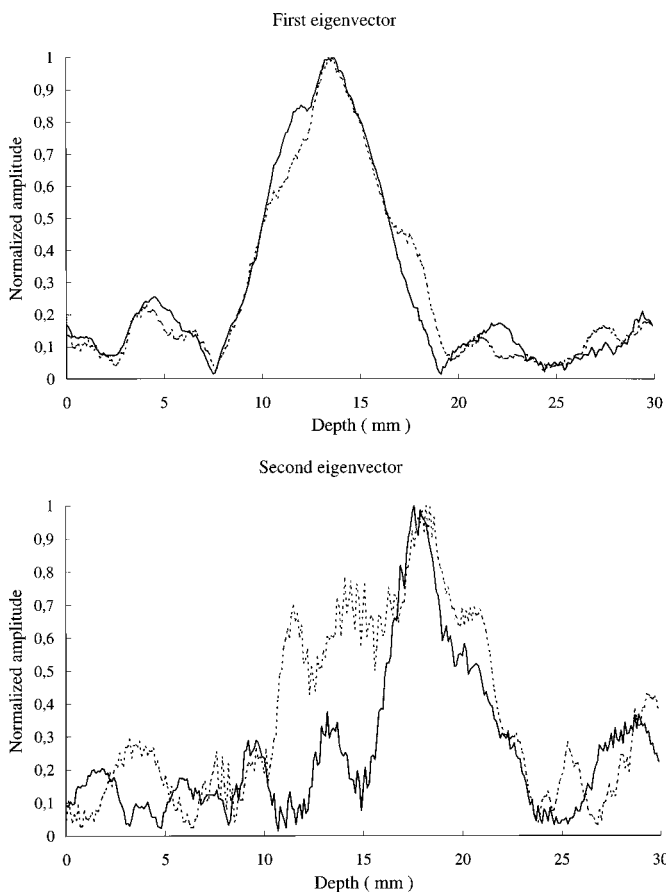


FIG. 15. Pressure field measured for transmission of the first eigenvector (a) and the second eigenvector (b) calculated with a nonaveraged transfer matrix (dot) and of a ten times averaged transfer matrix (solid) for surface waves of $h_{\text{rms}}=1.7$ mm.

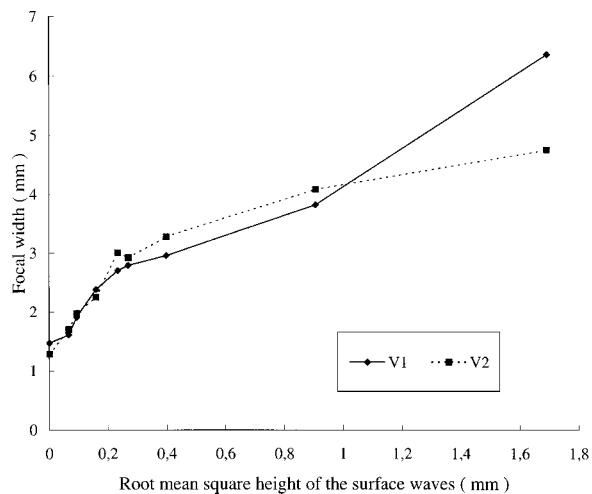


FIG. 16. Width of the focal spot versus the root mean square height of the surface waves measured for the ten times averaged transfer matrix.

scatterer is above noise even without averaging. Conversely, the focus pattern obtained with the second eigenvector calculated with K_1 is poor and noisy, whereas the focusing on the second wire is recovered with K_{10} [Fig. 15(b)].

The focus pressure pattern was measured for different h_{rms} . The -6 dB focal width was plot versus h_{rms} (Fig. 16). It varies from 1.2 mm to 6 mm for waves with $h_{\text{rms}}=1.7$ mm. For this height, the separation of the two wires corresponds to a resolution almost three times thinner than in free space. Such a resolution was necessarily obtained with a significant contribution of the wave reflected at the surface.

V. D.O.R.T. METHOD IN THE TIME DOMAIN

In the preceding sections, all of the results were obtained with the eigenvectors calculated at the central frequency of the transducers. Only a small part of the information contained in the inter-element impulse response functions has been used. In fact, decomposition of the time reversal operator can be done at any frequency. In order to get temporal signals, it would be natural to calculate the eigenvectors in the whole band of the transducers and to perform an inverse Fourier transform of the eigenvector function of frequency. In fact, this operation is nontrivial. The main reason is that the scatterers' reflectivity generally depends on frequency, so that at one frequency the first eigenvector can be associated to one scatterer while it is associated to another one at another frequency. However, if the strengths of the scatterers are different enough then the first eigenvector may correspond to the same scatterer in the whole frequency band of the transducers. In this case, it is possible to build temporal signals from the eigenvectors. If the first eigenvector corresponds to one pointlike scatterer, then the temporal signal will provide the impulse Green's function connecting the scatterer with the array. The details of this procedure will be discussed in another paper entirely devoted to what we call the extended D.O.R.T. method.

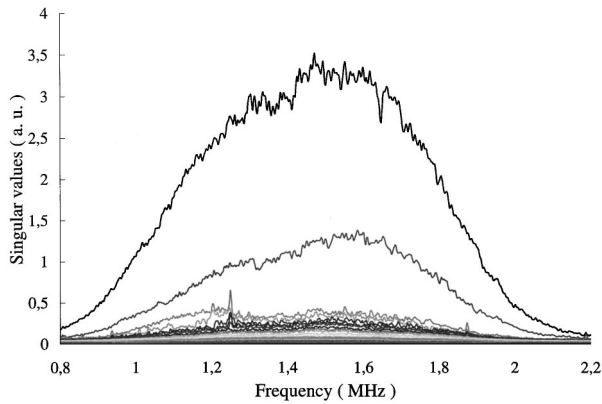


FIG. 17. Singular values of the transfer matrix versus frequency.

A. Construction of the temporal Green's functions

The abovementioned conditions are satisfied in the following example. The array of transducers and the waveguide are the same as in the Introduction. The range of the scatterers is 400 mm, the distance between the scatterers is 2 mm, and their reflectivities differ by a factor of 3 in the frequency band of the transducers. The SVD of the transfer matrix is calculated at each frequency of the discrete spectrum from 0.8 to 2.2 MHz. The singular values distribution versus frequency is shown Fig. 17: two singular values are apart from the 58 noise singular values and well separated from each other.

The impulse response function from the strong scatterer to the array can be reconstructed from the eigenvectors $\sqrt{\lambda_1(\omega)}V_1(\omega)$. Assuming the reflectivity of the scatterer is independent of frequency, this response is the temporal Green's function connecting the scatterer to the array convoluted by the acousto-electrical response of the transducer (Fig. 18, top). The same procedure applied to $\sqrt{\lambda_2(\omega)}V_2(\omega)$ provides the impulse Green's function from the second scatterer to the array (Fig. 18, bottom). This result is of particular interest in a complex propagating medium like a waveguide. Indeed, the low signal-to-noise ratio due to the length of the multiple path and the complexity of the echographic response of scatterer due to the double paths along the guide

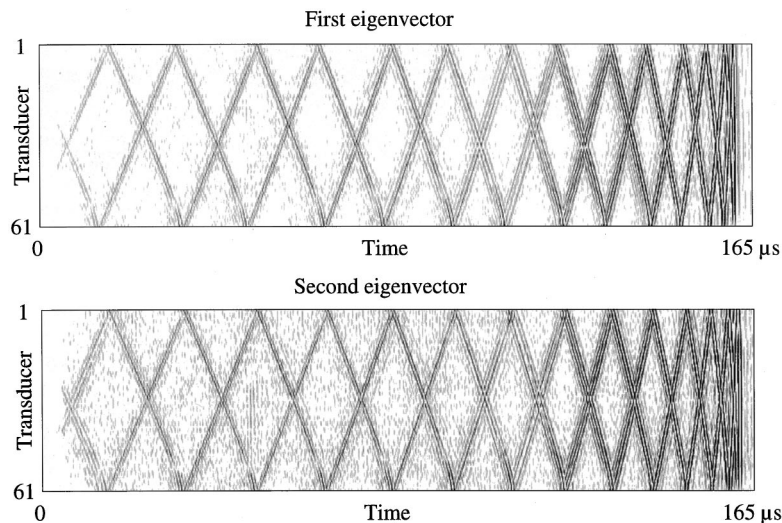


FIG. 18. Signals reconstructed from the first eigenvector (a) and from the second eigenvector (b). These signals correspond to the impulse response from each wire to the array.

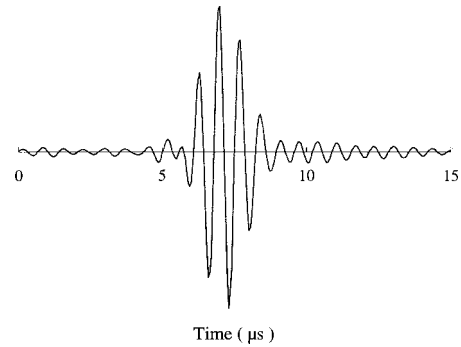


FIG. 19. Time domain compression: signal received at the position of the first wire after transmission of the first temporal eigenvector.

renders the determination of the impulse responses of the scatterers very difficult.

B. Selective focusing in the pulse mode

These signals are then transmitted from the array and the so-produced field is recorded along a line at the initial depth of the wires. One can observe an excellent temporal compression at the position of the wires: The transmitted signals are 165 μs long while the signal received at the wire position is a pulse 3 μs long (Fig. 19). The transverse peak pressure pattern of the first and second eigenvectors at the depth of the wire (Fig. 20) can be compared with the one obtained in monochromatic transmission (Sec. I, Fig. 4). The improvement in spatial focusing is undeniable (Fig. 21). The secondary lobes decrease to -30 dB while in the monochromatic transmission they remained around -18 dB.

VI. CONCLUSION

The echographic detection of scatterers in a simple water waveguide was studied. It was shown that the D.O.R.T. method provides information on the scattering medium that was not yet available. Taking advantage of the multiple reflections at the guide interfaces, the method was used to separate the signal coming from different scatterers and then to focus a wave field at anyone of them. The obtained resolution was nine times thinner than the free-space diffraction

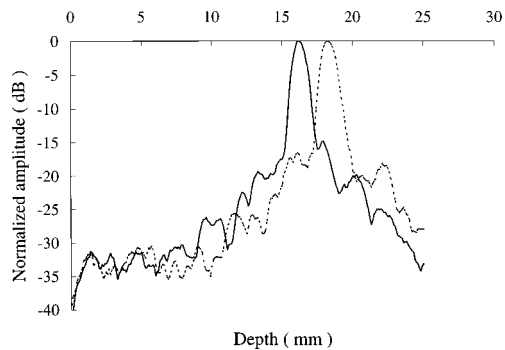


FIG. 20. Maximum of the pressure field measured at the depth of the wires across the guide after transmission of eigenvectors 1 and 2.

prediction. The method was also applied to the detection of a scatterer near the water/air interface, the distance under which the scatterer is no more detectable was shown to be less than $\lambda/5$ at a range of 400λ .

The efficiency of the method in a nonstationary guide with surface waves at the water/air interface was studied. For high waves ($kh_{\text{rms}}=10$), averaging of the transfer matrix allowed to reduce the noise singular values and to keep a resolution almost three times thinner than in free space. Finally, it was shown that a combination of the eigenvectors found at each frequency provided the impulse responses of each scatterer to the array.

These experimental results open several axis of research. The D.O.R.T. method could be applied to nondestructive testing in solid waveguides. This is of particular interest for defects that are close to the interfaces. The results presented in a nonstationary guide are promising and motivate further studies of underwater applications such as mine countermea-

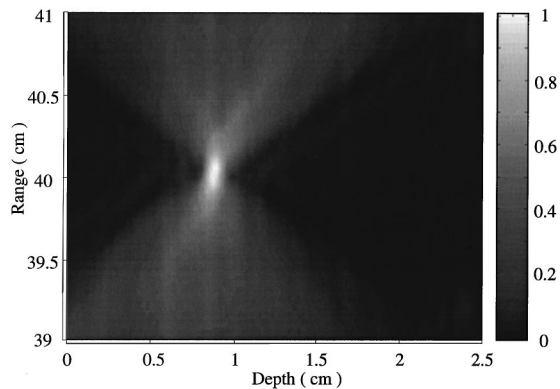


FIG. 21. 2D map of the maximum of the pressure field measured after transmission of the first eigenvector.

asures. A perturbation analysis of the transfer matrix in the presence of surface waves should be carried on. The time domain D.O.R.T. method could be used in detection to reduce sidelobe effects such as false location problem. Furthermore, the ability to achieve spatial and temporal compression may be applied to acoustic communication in shallow water.

ACKNOWLEDGMENTS

We wish to express our gratitude to Julien de Rosny for programming the procedures that allowed us to operate the electronic devices in a very convenient manner. This research was supported by the DRET Contract No. 96-1213.

- ¹A. Parvulescu and C. S. Clay, "Reproducibility of signal transmissions in the ocean," *Radio Electron. Eng.* **29**, 223–238 (1965).
- ²A. Parvulescu, "Matched—signal ('MESS') processing by the ocean," *J. Acoust. Soc. Am.* **98**, 943–960 (1995).
- ³C. Draeger and M. Fink, "One-channel time reversal of elastic waves in a chaotic 2D silicon cavity," *Phys. Rev. Lett.* **79**, 407–410 (1997).
- ⁴C. S. Clay, "Optimum time domain signal transmission and source location in a waveguide," *J. Acoust. Soc. Am.* **81**, 660–664 (1987).
- ⁵S. Li and C. S. Clay, "Optimum time domain signal transmission and source location in a waveguide: Experiments in an ideal wedge waveguide," *J. Acoust. Soc. Am.* **82**, 1409–1417 (1987).
- ⁶M. Fink, C. Prada, and F. Wu, "Self focusing in inhomogeneous media with time reversal acoustic mirrors," *Proc. IEEE Ultrason. Symp.* 1989, edited by B. R. McAvoy, Vol. 2, pp. 681–686 (1989).
- ⁷D. R. Jackson and D. R. Dowling, "Phase conjugation in underwater acoustics," *J. Acoust. Soc. Am.* **89**, 171–181 (1991).
- ⁸P. Roux, B. Roman, and M. Fink, "Transmissions acoustiques sous-marines dans les milieux à petits fonds: application du miroir à retournement temporel," 3^{ième} journées d'Etude en Acoustique Sous-Marine, Brest (1995).
- ⁹P. Roux, B. Roman, and M. Fink, "Time-reversal in an ultrasonic waveguide," *Appl. Phys. Lett.* **70**, 1811–1813 (1997).
- ¹⁰W. A. Kuperman, W. S. Hodgkiss, H. C. Song, T. Akal, C. Ferla, and D. R. Jackson, "Phase conjugation in the ocean: Experimental demonstration of an acoustic time-reversal mirror," *J. Acoust. Soc. Am.* **103**, 25–40 (1998).
- ¹¹C. Prada and M. Fink, "Eigenmodes of the time reversal operator: A solution to selective focusing in multiple target media," *Wave Motion* **20**, 151–163 (1994).
- ¹²C. Prada, J. L. Thomas, and M. Fink, "The iterative time reversal process: Analysis of the convergence," *J. Acoust. Soc. Am.* **97**, 62–71 (1995).
- ¹³C. Prada, S. Manneville, D. Spoliansky, and M. Fink, "Decomposition of the time reversal operator: Detection and selective focusing on two scatterers," *J. Acoust. Soc. Am.* **99**, 2067–2076 (1996).
- ¹⁴C. Prada and M. Fink, "Separation of interfering acoustic scattered signals using the invariant of the time-reversal operator. Application to Lamb waves characterization," *J. Acoust. Soc. Am.* **104**, 801–807 (1998).
- ¹⁵G. Bienvu and L. Kopp, "Optimality of high resolution array processing using the eigensystem approach," *IEEE Trans. Acoust., Speech, Signal Process.* **31**, 1235–1247 (1983).
- ¹⁶Ralph O. Schmidt, "Multiple Emitter Location and Signal Parameter Estimation," *IEEE Trans. Antennas Propag.* **AP-34**, 276–281 (1986).
- ¹⁷A. B. Baggeroer, W. A. Kuperman, and P. N. Mikhalevsky, "An overview of matched field methods in ocean acoustics," *IEEE J. Ocean Eng.* **18**, 401–424 (1993).